High mobility MOCVD β-Ga_2O_3 epitaxy with fast growth rate using trimethylgallium

Lingyu Meng,[1,*], Zixuan Feng[1] A F M Anhar Uddin Bhuiyan[1], and Hongping Zhao[1,2,‡]

[1]*Department of Electrical and Computer Engineering, The Ohio State University, Columbus, OH 43210, USA*

[2]*Department of Materials Science and Engineering, The Ohio State University, Columbus, OH 43210, USA*

[*]Email: meng.480@osu.edu

[‡]Corresponding Author Email: zhao.2592@osu.edu

Abstract

In this work, metalorganic chemical vapor deposition (MOCVD) of (010) β-Ga_2O_3 with fast growth rates was investigated using trimethylgallium (TMGa) as the gallium (Ga) precursor. Key growth parameters including precursor/carrier gas flow, growth temperature, chamber pressure, and group VI/III molar flow ratio were systematically mapped. Surface morphology and charge transport properties of the homo-epi (010) β-Ga_2O_3 thin films were probed to correlate with the crystalline quality. The growth rate of (010) β-Ga_2O_3 thin film increases as the TMGa flow rate increases, and high quality epi-film is achievable with fast growth rate up to ~ 3 μm/hr. By tuning the n-type dopant silane flow rate, the net charge carrier concentration was tuned from ~10^{16} to 10^{19} cm^{-3}. Room temperature mobility as high as 190 $cm^2/V{\cdot}s$ was measured for a sample grown with growth rate of 2.95 μm/hr and electron concentration of 1.8×10^{16} cm^{-3}. Temperature dependent Hall measurement revealed a peak mobility value of ~3400 $cm^2/V{\cdot}s$ at 53 K. The extracted low compensation level of N_A ~ 1.5×10^{15} cm^{-3} indicates the high purity of the MOCVD growth of (010) β-Ga_2O_3 film using TMGa as the Ga precursor. Quantitative

secondary-ion mass spectroscopy characterization revealed a relatively high C concentration of $7x10^{16}$ cm^{-3}, indicating C does not serve as a compensator or a donor in MOCVD grown β-Ga_2O_3. The results from this study demonstrate the feasibility to grow high quality Ga_2O_3 thin films with fast growth rates, critical for developing high power electronic device technology.

Keywords: Ultra-wide bandgap semiconductor, Ga_2O_3, MOCVD epitaxy, charge transport

I. Introduction

Ga_2O_3 represents an emerging semiconductor material, and the monoclinic β-phase is the most thermally stable one among several known phases (α, β, γ, δ, and ε/κ). [1] Due to its ultra-wide bandgap energy (~4.8 eV) located in the deep ultraviolet (DUV) spectrum [1, 2], β-Ga_2O_3 has been considered as a promising candidate in optoelectronic and photonic applications such as solar-blind detection [3–5] and transparent conductive oxide. [6, 7] Recent demonstrations on β-Ga_2O_3 based diodes and transistors, [8–10] on the other hand, have expanded its application for power switching, taking advantage of the high predicted critical field of 8MV/cm - exceeding most existing wide bandgap semiconductors. [8] In addition, the wide-range and controllable n-type doping [11–15], epitaxy of semi-insulating layer [16, 17], and the commercially available high quality bulk substrates [7] promise its applications for high power switching/radio-frequency (RF) electronics. [8, 18]

Thin film epitaxy of Ga_2O_3 has advanced significantly in the past decade that provides high-quality, well-controlled thin films for device design and device demonstration. The most common deposition methods include pulsed laser deposition (PLD), [19–21] atomic layer deposition (ALD), [22–24] halide vapor phase epitaxy (HVPE), [12, 25–27]

molecular beam epitaxy (MBE) [13, 28–30] and chemical vapor depositions (CVD). [11, 14, 15, 31–38] Thus far, metalorganic chemical vapor deposition (MOCVD) is considered as the most promising growth technique that produces high crystalline quality β-Ga_2O_3 thin films and Ga_2O_3/AlGaO heterostructures. Soon after the first demonstrations of MOCVD β-Ga_2O_3 on (010) and (100) native substrates, [11, 31] high-quality (010) β-Ga_2O_3 thin films with room temperature (RT) mobility approaching theoretically predicted limit of ~200 $cm^2/V.s$ was demonstrated. [14, 38-40] The low temperature (LT) peak mobility values ranged from ~5000 up to 23000 $cm^2/V.s$, which indicates very high purity of the materials and the extremely low charge compensation level ($<10^{15}$ cm^{-3}) in the MOCVD β-Ga_2O_3. [14, 38, 40–42] This shows the great promise of (010) β-Ga_2O_3 for high power electronics where extreme breakdown voltage is required. MOCVD homoepitaxy of (100) β-Ga_2O_3 achieved improved crystalline quality when off-axis substrates with optimal off-cut angle were used. [33–35, 43] The close matching between the off-cut steps on the growth surface and the adatom diffusion length greatly promotes the step-flow growth mode, which in turn suppresses the structural defects formation. [34, 43] N-type dopants such as Si, Sn and Ge have been demonstrated as effective shallow donors in MOCVD β-Ga_2O_3, [11, 14, 32, 44] whereas in-situ MOCVD growth of Mg-doped β-Ga_2O_3 has shown effective charge compensation and the formation of semi-insulating layer. [16, 17] The doping capability in MOCVD β-Ga_2O_3 has granted great opportunity and flexibility in device design and fabrication.

Thus far, majority of the demonstrations of β-Ga_2O_3 vertical devices with thick drift layer are based on HVPE grown materials, because of its capability to grow β-Ga_2O_3 with relatively fast growth rates > 10 μm/h. [45, 46] However, HVPE growth with fast growth

rate tends to cause severe surface roughness with surface steps and pits, [26, 47] and therefore it requires a chemical-mechanical polishing (CMP) process for device fabrication. [12] On the other hand, MBE β-Ga_2O_3 typically has a slow growth rate at ~0.2 μm/h due to the limited evaporation of metal cell and desorption under ultra-high vacuum. [13, 28] Particularly, the suboxide (Ga_2O) formation and its consequent desorption from deposition surface also limit the MBE growth temperatures and the Ga/O flux ratio. [30] Recently, a metal-oxide catalyzed epitaxy (MOCATAXY, also known as metal exchange catalyzed epitaxy MEX-CAT) was proposed to address the limited growth rates in MBE β-Ga_2O_3, in which intermediate metal and oxides such as In/In_2O_3 are applied on the growth surface as a catalyst for the deposition of Ga_2O_3, with growth rate of 0.3 μm/h. [48–51] Suboxide MBE (S-MBE) was also proposed by using suboxide molecular beams to avoid the desorption reactions on the growth surface in conventional MBE. [52] Enhanced growth rates up to 1.5 μm/h was demonstrated by S-MBE β-Ga_2O_3 on (010) orientation. [50] However, it is still challenging to develop thick Ga_2O_3 layers by using MBE growth technique.

The typical growth rate of MOCVD β-Ga_2O_3 ranges between 0.2-1.0 μm/h, using triethylgallium (TEGa) as the Ga precursor. [34, 35, 38, 40] Note that MOCVD growth of GaN commonly uses trimethylgallium (TMGa) as the Ga precursor for high temperature thick layer growth, and TEGa for low temperature thin layer growth at the nm scale. [53–55] TMGa has a higher vapor pressure and faster reaction kinetics as compared to TEGa, due to the active moiety of the organic ligand. [56] Previously, MOCVD growth of β-Ga_2O_3 using TMGa as Ga precursor in a close coupled showerhead reactor has demonstrated fast growth rates up to 9.8 μm/h with a high TMGa molar flow rate. [57]

However, the surface morphology or electrical transport characteristics was not studied in these materials. Recently, MOCVD growth of β-Ga_2O_3 using TMGa as precursor reported film growth rate of 1.5 μm/h, surface RMS of 1.8 nm, room temperature mobility of 125 cm^2/Vs with carrier concentration of 1.5 $x10^{16}$ cm^{-3}, and low temperature peak mobility of 23000 cm^2/V s at 32 K. [42]

In this work, a systematic growth study was performed to investigate the growth window of MOCVD (010) β-Ga_2O_3 using TMGa precursor in a far injection showerhead reactor, in which record room temperature mobility of (010) β-Ga_2O_3 with TEGa as precursor has been demonstrated. The key focus of this study is to explore the growth conditions that enable high quality β-Ga_2O_3 growth with fast growth rates beyond what has been demonstrated.

II. Experimental Section

The β-Ga_2O_3 films were grown via MOCVD on Fe-doped semi-insulating (010) native β-Ga_2O_3 substrates (5x5 mm^2, commercially acquired from Novel Crystal Technology, Inc.). The lightly n-doped β-Ga_2O_3 homoepitaxial thin films were grown with varying growth temperature from 700 °C to 950 °C, and chamber pressure from 20 torr to 100 torr. TMGa and pure O_2 were used as Ga and O precursors, respectively. Ar was used as the carrier gas. O_2 flow rate was tuned from 500 ~ 1000 SCCM, and TMGa molar flow rate was varied between 48 μmol/min and 116 μmol/min. Silane was used as the n-type Si doping source. Prior to loading the substrate in the MOCVD chamber, the substrates were cleaned by Acetone, IPA and DI-water. Before the growth starts, high temperature in-situ annealing at 920 °C was performed for 5 mins under O_2 atmosphere. Atomic force microscopy (AFM, Bruker AXS Dimension Icon, tapping mode, the radius of uncoated

tip=8 nm) and field emission (FE) scanning electron microscopy (FESEM, FEI Helios 650) were used to characterize the surface morphology of the as-grown samples. The film thicknesses were estimated by measuring the film thicknesses of β-Ga_2O_3 films grown on the co-loaded sapphire substrates through the cross-sectional FESEM imaging. Room temperature carrier transport characteristics were measured using van der Pauw Hall measurement setup (Ecopia HMS 3000, magnetic field=0.975 T, sample size is 5x5 mm^2). Ti/Au (30/100 nm) contacts were deposited on the four corners of the sample to form Ohmic contacts which were verified via I-V measurement. Temperature-dependent Hall measurements were performed on selected samples using Lakeshore Series 8400 HMS system (magnetic field=0.7 T, wire-bonding contacts).

III. Results and Discussion

A systematic MOCVD growth condition mapping was performed for β-Ga_2O_3 homoepitaxy using TMGa as the precursor. The key growth parameters and sample information were listed in Table 1. The dependence of film growth on temperature was studied by varying the growth temperature from 700, 880, to 950 °C (#309, #307, and #310), with a fixed TMGa molar flow rate at 58 μmol/min, growth pressure of 60 torr and O_2 flow rate of 800 SCCM. The results indicate that the fastest growth rate of ~ 2.8 μm/h was achieved at 880 °C. At relatively low growth temperature (e.g. 700 °C), the β-Ga_2O_3 growth rate is limited by chemical reaction rate. At high growth temperature (e.g. 950 °C), gas phase reaction and surface desorption can become limiting factors that prevent achieving fast growth rates. Fig. 1 shows the surface morphologies of the β-Ga_2O_3 samples (#309, #307, and #310) grown at different temperatures via SEM and AFM imaging, revealing homogenous growth surfaces, albeit with ~ 4X faster growth rate as compared to

films grown using TEGa. [38, 40] It is worth noting that films grown under high temperature at 950 °C show effective conduction based on Hall measurements. This indicates that films grown at lower temperatures with TMGa as precursor are likely to have strong compensation.

From previous MOCVD β-Ga_2O_3 growth using TEGa as precursor, it has been found that growth pressure and precursor flow velocity have a significant impact on β-Ga_2O_3 growth rate since gas phase reaction between the precursors occurs before reaching to the growth surface. [38] It is expected that gas phase reaction between TMGa and oxygen can play an important role for MOCVD growth of β-Ga_2O_3 using TMGa as the Ga precursor. In this work, growth studies were performed with different growth pressure at 20 (#314), 60 (#313) and 100 (#315) torr, with the same growth temperature (950 °C), TMGa molar flow rate (48 μmol/min) and O_2 flow rate (800 SCCM). The growth rate varies significantly in these samples, with a relatively fast growth rate of 3.29 μm/h at 20 torr and a relatively slow growth rate of 1.57 μm/h at 100 Torr. As shown in Fig. 2(a), non-flat surface is observed from the sample grown at 20 torr, indicating non-ideal layer-by-layer growth mode in local regions. In contrast, as shown in Fig. 2(b)-(d), films grown at 60 and 100 torr show smooth surfaces with low RMS values of 1.23 nm and 2.05 nm. This study reveals the tradeoff between the MOCVD β-Ga_2O_3 growth rate and surface smoothness that can be achieved.

The dependence of MOCVD β-Ga_2O_3 growth on precursor flow rate was investigated by varying the TMGa molar flow rate and O_2 flow rate, respectively. As listed in Table 1, from samples (#320, #326, #322 and #319), the film growth rate increases monotonically as TMGa molar flow rate increases with a fixed O_2 flow rate of 800 SCCM. In contrast,

the film growth rate decreases with increasing of oxygen flow rate (#321, #322, and #323) with a fixed TMGa flow rate of 87 μmol/min. Under oxygen rich growth conditions, the film growth rate is limited by the available Ga precursors reaching the growth surface. With a higher oxygen flow rate, the promoted gas phase reaction reduces the Ga precursor participating the chemical reaction at the growth surface.

Significantly enhanced growth rates of 6.71 (6.24) μm/h were achieved with TMGa molar flow rate of 116 (87) μmol/min and O_2 flow rate of 800 (500) SCCM for Sample #319 (#321). The characterization of surface morphologies, as shown in Fig. 3, indicates that higher TMGa molar flow rate > 87 μmol/min (Fig. 3 (c-d)) can lead to the formation of macroscopic defects on the growth surface, despite similar RMS values (1.28-2.12 nm) were measured from AFM imaging. From Fig. 4, the increase of O_2 flow rate from 500 to 1000 SCCM has minimum impact on surface morphology from both SEM and AFM imaging.

Room temperature Hall measurements on the series of MOCVD Si-doped β-Ga_2O_3 samples reveal that relatively higher silane flow rate is required to achieve effective conduction as the film growth rate increases. As listed in Table 1, for the samples (#329, #326, #327, #335, #336, and #337) grown with TMGa molar flow rate of 58 μmol/min, O_2 flow rate of 800 SCCM, growth pressure of 60 torr, and growth temperature of 950 °C, a wide range of doping concentration ($1.8x10^{16}$ – $3.8x10^{19}$ cm^{-3}) was achieved by tuning the silane flow rate from 0.05 – 166.4 nmol/min. The film growth rates of these samples range between 2.67-3.17 μm/h. Specifically, for Sample #329, a room temperature mobility of 190 cm^2/Vs was achieved with carrier concentration of 1.8×10^{16} cm^{-3}, which is close to the highest room temperature mobility value reported for MOCVD grown β-Ga_2O_3 using

TEGa as precursor. [40] The surface morphology of Sample #329 was characterized by both SEM and AFM as shown in Fig. 5, revealing smooth surface with low RMS of 1.66 nm.

Figure 6 plots the room temperature mobility as a function of doping concentration for the series of samples discussed above, as compared to the reported values from β-Ga_2O_3 films grown via different growth techniques. The corresponding growth rates are also listed. [12-14, 28, 32, 35, 38-40, 42, 44, 47, 58-63]. In general, MOCVD grown β-Ga_2O_3 films show relatively higher mobilities as compared to the films grown by MBE, PLD or HVPE. For the films grown in this work with growth rate of ~3 μm/h, the results reveal similar room temperature mobility values as compared to the highest reported values grown using TEGa at growth rate of ~ 1.0 μm/h. [38] This demonstrates the feasibility to maintain high crystalline quality of MOCVD (010) β-Ga_2O_3 films using TMGa precursor with faster growth rates.

Temperature-dependent Hall measurement was performed on a selected sample (#329) to probe the carrier transport properties as a function of temperature, as plotted in Fig. 7(a). To extract the donor characteristics, the carrier concentration vs. temperature data were fitted by using the two-donor model. [14, 64] The charge neutrality equation can be expressed as the following:

$$n + N_A = \frac{N_{d1}}{1 + 2e^{-(E_{d1} - E_F)/k_B T}} + \frac{N_{d2}}{1 + 2e^{-(E_{d2} - E_F)/k_B T}}$$

In this equation, N_A is the acceptor concentration, assuming full ionization among all temperatures, and N_{d1} and N_{d2} are the concentrations of the two donors whereas E_{d1} and

E_{d2} are the corresponding activation energies of the donors. Details on the fitting and process of donor characteristics extraction are included in the supplemental material. Based on the carrier concentration fitting, two donor states were extracted with activation energy of E_{d1} = 36 meV and E_{d2} = 130 meV and the corresponding extracted concentrations of N_{d1} ~1.8×10^{16} cm^{-3} and N_{d2} ~ 5×10^{15} cm^{-3}, respectively. The shallow donor state commonly refers to the Si occupying the tetrahedral Ga(I) site, whereas the origin of the second donor state is still unclear with possible defects related to antisites/interstitials or impurities such as hydrogen, or Si on the octahedrally coordinated Ga(II) site. [65]

Figure 7(b) plotted the temperature dependent electron mobilities and the fitting took into account the polar optical phonon (POP), acoustic (phonon) deformation potential (ADP), ionized impurity (II), and neutral impurity (NI) scattering processes. The peak mobility of 3425 cm^2/Vs was measured at 53 K, and the extracted charge compensation was N_A ~ 1.45×10^{15} cm^{-3}. Here, in order to quantitatively evaluate the accuracy on the fitting, the parameter R-squared (square of the correlation coefficient) is included to describe the deviation of the fittings from the experimental data. The deviation for carrier mobility $\mu(T)$ fitting is $R^2 = 0.981$ and for carrier density $\log n(1/T)$ fitting is $R^2 = 0.999$, indicating both fittings have very low deviations. The low compensation level indicates the great potential to achieve active layer with controllable n type doping at mid-high x10^{15} cm^{-3}- critical for devices targeting for multi-kV breakdown voltages.

To probe the impurity concentrations and correlate with the charge transport properties, quantitative secondary-ion mass spectroscopy (SIMS) was performed on the same sample (#329). As shown in Fig. 8, the Si impurity concentration of ~1.8×10^{16} cm^{-3} matches with the charge concentration extracted from the temperature-dependent carrier

transport characteristics. The background carbon (C) impurity level (~ 7×10^{16} cm^{-3}) was found to be above the detection limit (5×10^{16} cm^{-3}) of SIMS characterization. This indicates a higher C incorporation from MOCVD β-Ga_2O_3 growth using TMGa as the precursor. In MOCVD growth of GaN, background carbon incorporation was found as one of the main sources of charge compensation to the n-type dopants. One expects similar role of C in MOCVD β-Ga_2O_3 may exist. Combining the charge transport characteristics and quantitative SIMS, C does not serve as a shallow donor or a direct compensation center, since the free charge carrier concentration matches well with the Si concentration. However, it is possible that the formation of C-H complexes neutralize the C impurity, as predicted from DFT calculation [66]. Further investigations are required to understand the role of C in MOCVD β-Ga_2O_3 films using TMGa as precursor.

IV. Conclusions

In conclusion, MOCVD growth condition was systematically mapped to correlate the growth temperature, chamber pressure, TMGa molar flow rate, and O_2 flow rate with the β-Ga_2O_3 thin film surface morphology, growth rate, and charge transport properties. The study reveals the tradeoff between the film growth rate and crystalline quality in MOCVD grown (010) β-Ga_2O_3 thin films using TMGa as precursor. Superior electron transport properties were demonstrated in β-Ga_2O_3 films with growth rate at ~ 3 μm/h. With carrier concentration of 1.8×10^{16} cm^{-3}, room temperature mobility of 190 cm^2/Vs was achieved, approaching the theoretically predicted limit. A wide range of doping was demonstrated, indicating the great promise to develop β-Ga_2O_3 power devices using MOCVD growth technique and TMGa as precursor.

Acknowledgement: The authors thank the financial support from the Air Force Office of Scientific Research FA9550-18-1-0479 (AFOSR, Dr. Ali Sayir), and the NSF (Grant No. 1810041, No. 2019753).

References:

(1) Tippins, H. H. Optical Absorption and Photoconductivity in the Band Edge of β-Ga_2O_3. *Phys. Rev.* **1965**, *140*, A316–A319.
(2) Onuma, T.; Fujioka, S.; Yamaguchi, T.; Higashiwaki, M.; Sasaki, K.; Masui, T.; Honda, T. Correlation between blue luminescence intensity and resistivity in β-Ga_2O_3 single crystals. *Appl. Phys. Lett.* **2013**, *103*, 041910.
(3) Oshima, T.; Okuno, T.; Arai, N.; Suzuki, N.; Ohira, S.; Fujita, S. Vertical Solar-Blind Deep-Ultraviolet Schottky Photodetectors Based on β-Ga_2O_3 Substrates. *Appl. Phys. Express* **2008**, *1*, 011202.
(4) Pratiyush, A. S.; Krishnamoorthy, S.; Kumar, S.; Xia, Z.; Muralidharan, R.; Rajan, S.; Nath, D. N. Demonstration of zero bias responsivity in MBE grown β-Ga_2O_3 lateral deep-UV photodetector. *Jpn. J. Appl. Phys.* **2018**, *57*, 060313.
(5) Pratiyush, A. S.; Krishnamoorthy, S.; Muralidharan, R.; Rajan, S.; Nath, D. N. 16 - Advances in Ga_2O_3 solar-blind UV photodetectors. In *Gallium Oxide*; Pearton, S., Ren, F., Mastro, M., Eds.; Metal Oxides; Elsevier, **2019**; pp 369–399.
(6) Aida, H.; Nishiguchi, K.; Takeda, H.; Aota, N.; Sunakawa, K.; Yaguchi, Y. Growth of β-Ga_2O_3 Single Crystals by the Edge-Defined, Film Fed Growth Method. *Jpn. J. Appl. Phys.* **2008**, *47*, 8506.
(7) Kuramata, A.; Koshi, K.; Watanabe, S.; Yamaoka, Y.; Masui, T.; Yamakoshi, S. High-quality β-Ga_2O_3 single crystals grown by edge-defined film-fed growth. *Jpn. J. Appl. Phys.* **2016**, *55*, 1202A2.
(8) Higashiwaki, M.; Sasaki, K.; Kuramata, A.; Masui, T.; Yamakoshi, S. Gallium oxide (Ga_2O_3) metal-semiconductor field-effect transistors on single-crystal β-Ga_2O_3 (010) substrates. *Appl. Phys. Lett.* **2012**, *100*, 013504.
(9) Higashiwaki, M.; Sasaki, K.; Kamimura, T.; Hoi Wong, M.; Krishnamurthy, D.; Kuramata, A.; Masui, T.; Yamakoshi, S. Depletion-mode Ga_2O_3 metal-oxide-semiconductor field-effect transistors on β-Ga_2O_3 (010) substrates and temperature dependence of their device characteristics. *Appl. Phys. Lett.* **2013**, *103*, 123511.
(10) Sasaki, K.; Higashiwaki, M.; Kuramata, A.; Masui, T.; Yamakoshi, S. Ga_2O_3 Schottky Barrier Diodes Fabricated by Using Single-Crystal β-Ga_2O_3 (010) Substrates. *IEEE Electron Device Lett.* **2013**, *34*, 493–495.
(11) Baldini, M.; Albrecht, M.; Fiedler, A.; Irmscher, K.; Klimm, D.; Schewski, R.; Wagner, G. Semiconducting Sn-doped β-Ga_2O_3 homoepitaxial layers grown by metal organic vapour-phase epitaxy. *J. Mater. Sci.* **2016**, *51*, 3650–3656.
(12) Goto, K.; Konishi, K.; Murakami, H.; Kumagai, Y.; Monemar, B.; Higashiwaki, M.; Kuramata, A.; Yamakoshi, S. Halide vapor phase epitaxy of Si doped β-Ga_2O_3 and its electrical properties. *Thin Solid Films* **2018**, *666*, 182–184.

(13) Ahmadi, E.; Koksaldi, O. S.; Kaun, S. W.; Oshima, Y.; Short, D. B.; Mishra, U. K.; Speck, J. S. Ge doping of β-Ga_2O_3 films grown by plasma-assisted molecular beam epitaxy. *Appl. Phys. Express* **2017**, *10*, 041102.
(14) Zhang, Y.; Alema, F.; Mauze, A.; Koksaldi, O. S.; Miller, R.; Osinsky, A.; Speck, J. S. MOCVD grown epitaxial β-Ga_2O_3 thin film with an electron mobility of 176 cm^2/V s at room temperature. *APL Mater.* **2019**, *7*, 022506.
(15) Rafique, S.; Han, L.; Neal, A. T.; Mou, S.; Boeckl, J.; Zhao, H. Towards High-Mobility Heteroepitaxial β-Ga_2O_3 on Sapphire − Dependence on The Substrate Off-Axis Angle. *Phys. Status Solidi (A)* **2018**, *215*, 1700467.
(16) Feng, Z.; Bhuiyan, A. F. M. A. U.; Kalarickal, N. K.; Rajan, S.; Zhao, H. Mg acceptor doping in MOCVD (010) β-Ga_2O_3. *Appl. Phys. Lett.* **2020**, *117*, 222106.
(17) Mauze, A.; Zhang, Y.; Itoh, T.; Mates, T. E.; Peelaers, H.; Van de Walle, C. G.; Speck, J. S. Mg doping and diffusion in (010) β-Ga_2O_3 films grown by plasma-assisted molecular beam epitaxy. *J. Appl. Phys.* **2021**, *130*, 235301.
(18) Green, A. J.; Chabak, K. D.; Heller, E. R.; Fitch, R. C.; Baldini, M.; Fiedler, A.; Irmscher, K.; Wagner, G.; Galazka, Z.; Tetlak, S. E.; Crespo, A.; Leedy, K.; Jessen, G. H. 3.8-MV/cm Breakdown Strength of MOVPE-Grown Sn-Doped β-Ga_2O_3 MOSFETs. *IEEE Electron Device Lett.* **2016**, *37*, 902–905.
(19) Orita, M.; Hiramatsu, H.; Ohta, H.; Hirano, M.; Hosono, H. Preparation of highly conductive, deep ultraviolet transparent β-Ga_2O_3 thin film at low deposition temperatures. *Thin Solid Films* **2002**, *411*, 134–139.
(20) Leedy, K. D.; Chabak, K. D.; Vasilyev, V.; Look, D. C.; Boeckl, J. J.; Brown, J. L.; Tetlak, S. E.; Green, A. J.; Moser, N. A.; Crespo, A.; Thomson, D. B.; Fitch, R. C.; McCandless, J. P.; Jessen, G. H. Highly conductive homoepitaxial Si-doped Ga_2O_3 films on (010) β-Ga_2O_3 by pulsed laser deposition. *Appl. Phys. Lett.* **2017**, *111*, 012103.
(21) Matsuzaki, K.; Hiramatsu, H.; Nomura, K.; Yanagi, H.; Kamiya, T.; Hirano, M.; Hosono, H. Growth, structure and carrier transport properties of Ga_2O_3 epitaxial film examined for transparent field-effect transistor. *Thin Solid Films* **2006**, *496*, 37–41.
(22) Valet, M.; Hoffman, D. M. Synthesis of Homoleptic Gallium Alkoxide Complexes and the Chemical Vapor Deposition of Gallium Oxide Films. *Chem. Mater.* **2001**, *13*, 2135–2143.
(23) Dezelah; Niinistö, J.; Arstila, K.; Niinistö, L.; Winter, C. H. Atomic Layer Deposition of Ga_2O_3 Films from a Dialkylamido-Based Precursor. *Chem. Mater.* **2006**, *18*, 471–475.
(24) Choi, D.; Chung, K.-B.; Park, J.-S. Low temperature Ga_2O_3 atomic layer deposition using gallium tri-isopropoxide and water. *Thin Solid Films* **2013**, *546*, 31–34.
(25) Nomura, K.; Goto, K.; Togashi, R.; Murakami, H.; Kumagai, Y.; Kuramata, A.; Yamakoshi, S.; Koukitu, A. Thermodynamic study of β-Ga_2O_3 growth by halide vapor phase epitaxy. *J. Cryst. Growth* **2014**, *405*, 19–22.
(26) Murakami, H.; Nomura, K.; Goto, K.; Sasaki, K.; Kawara, K.; Thieu, Q. T.; Togashi, R.; Kumagai, Y.; Higashiwaki, M.; Kuramata, A.; Yamakoshi, S.; Monemar, B.; Koukitu, A. Homoepitaxial growth of β-Ga_2O_3 layers by halide vapor phase epitaxy. *Appl. Phys. Express* **2014**, *8*, 015503.
(27) Oshima, Y.; Víllora, E. G.; Shimamura, K. Halide vapor phase epitaxy of twin-free α-Ga_2O_3 on sapphire (0001) substrates. *Appl. Phys. Express* **2015**, *8*, 055501.

(28) Sasaki, K.; Kuramata, A.; Masui, T.; Víllora, E. G.; Shimamura, K.; Yamakoshi, S. Device-Quality β-Ga_2O_3 Epitaxial Films Fabricated by Ozone Molecular Beam Epitaxy. *Appl. Phys. Express* **2012**, *5*, 035502.
(29) Tsai, M.-Y.; Bierwagen, O.; White, M. E.; Speck, J. S. *β*-Ga_2O_3 growth by plasma-assisted molecular beam epitaxy. *J. Vac. Sci. Technol. A* **2010**, *28*, 354–359.
(30) Vogt, P.; Bierwagen, O. Reaction kinetics and growth window for plasma-assisted molecular beam epitaxy of Ga_2O_3: Incorporation of Ga vs. Ga_2O desorption. *Appl. Phys. Lett.* **2016**, *108*, 072101.
(31) Wagner, G.; Baldini, M.; Gogova, D.; Schmidbauer, M.; Schewski, R.; Albrecht, M.; Galazka, Z.; Klimm, D.; Fornari, R. Homoepitaxial growth of β-Ga_2O_3 layers by metal-organic vapor phase epitaxy. *Phys. Status Solidi (A)* **2014**, *211*, 27–33.
(32) Baldini, M.; Albrecht, M.; Fiedler, A.; Irmscher, K.; Schewski, R.; Wagner, G. Editors' Choice—Si- and Sn-Doped Homoepitaxial β-Ga_2O_3 Layers Grown by MOVPE on (010)-Oriented Substrates. *ECS J. Solid State Sci. Technol.* **2016**, *6*, Q3040.
(33) Fiedler, A.; Schewski, R.; Baldini, M.; Galazka, Z.; Wagner, G.; Albrecht, M.; Irmscher, K. Influence of incoherent twin boundaries on the electrical properties of β-Ga_2O_3 layers homoepitaxially grown by metal-organic vapor phase epitaxy. *J. Appl. Phys.* **2017**, *122*, 165701.
(34) Schewski, R.; Lion, K.; Fiedler, A.; Wouters, C.; Popp, A.; Levchenko, S. V.; Schulz, T.; Schmidbauer, M.; Bin Anooz, S.; Grüneberg, R.; Galazka, Z.; Wagner, G.; Irmscher, K.; Scheffler, M.; Draxl, C.; Albrecht, M. Step-flow growth in homoepitaxy of β-Ga_2O_3 (100)—The influence of the miscut direction and faceting. *APL Mater.* **2019**, *7*, 022515.
(35) Bin Anooz, S.; Grüneberg, R.; Wouters, C.; Schewski, R.; Albrecht, M.; Fiedler, A.; Irmscher, K.; Galazka, Z.; Miller, W.; Wagner, G.; Schwarzkopf, J.; Popp, A. Step flow growth of β-Ga_2O_3 thin films on vicinal (100) β-Ga_2O_3 substrates grown by MOVPE. *Appl. Phys. Lett.* **2020**, *116*, 182106.
(36) Rafique, S.; Karim, M. R.; Johnson, J. M.; Hwang, J.; Zhao, H. LPCVD homoepitaxy of Si doped β-Ga_2O_3 thin films on (010) and (001) substrates. *Appl. Phys. Lett.* **2018**, *112*, 052104.
(37) Rafique, S.; Han, L.; Tadjer, M. J.; Freitas, J. A.; Mahadik, N. A.; Zhao, H. Homoepitaxial growth of β-Ga_2O_3 thin films by low pressure chemical vapor deposition. *Appl. Phys. Lett.* **2016**, *108*, 182105.
(38) Feng, Z.; Anhar Uddin Bhuiyan, A. F. M.; Karim, M. R.; Zhao, H. MOCVD homoepitaxy of Si-doped (010) β-Ga_2O_3 thin films with superior transport properties. *Appl. Phys. Lett.* **2019**, *114*, 250601.
(39) Alema, F.; Zhang, Y.; Mauze, A.; Itoh, T.; Speck, J. S.; Hertog, B.; Osinsky, A. H_2O vapor assisted growth of β-Ga_2O_3 by MOCVD. *AIP Adv.* **2020**, *10*, 085002.
(40) Feng, Z.; Bhuiyan, A. F. M. A. U.; Xia, Z.; Moore, W.; Chen, Z.; McGlone, J. F.; Daughton, D. R.; Arehart, A. R.; Ringel, S. A.; Rajan, S.; Zhao, H. Probing Charge Transport and Background Doping in Metal-Organic Chemical Vapor Deposition-Grown (010) β-Ga_2O_3. *Phys. Status Solidi RRL* **2020**, *14*, 2000145.
(41) Alema, F.; Zhang, Y.; Osinsky, A.; Valente, N.; Mauze, A.; Itoh, T.; Speck, J. S. Low temperature electron mobility exceeding 10^4 cm^2/V s in MOCVD grown β-Ga_2O_3. *APL Mater.* **2019**, *7*, 121110.

(42) Seryogin, G.; Alema, F.; Valente, N.; Fu, H.; Steinbrunner, E.; Neal, A. T.; Mou, S.; Fine, A.; Osinsky, A. MOCVD growth of high purity Ga_2O_3 epitaxial films using trimethylgallium precursor. *Appl. Phys. Lett.* **2020**, *117*, 262101.
(43) Schewski, R.; Baldini, M.; Irmscher, K.; Fiedler, A.; Markurt, T.; Neuschulz, B.; Remmele, T.; Schulz, T.; Wagner, G.; Galazka, Z.; Albrecht, M. Evolution of planar defects during homoepitaxial growth of β-Ga_2O_3 layers on (100) substrates—A quantitative model. *J. Appl. Phys.* **2016**, *120*, 225308.
(44) Alema, F.; Seryogin, G.; Osinsky, A.; Osinsky, A. Ge doping of β-Ga_2O_3 by MOCVD. *APL Mater.* **2021**, *9*, 091102.
(45) Hu, Z.; Nomoto, K.; Li, W.; Tanen, N.; Sasaki, K.; Kuramata, A.; Nakamura, T.; Jena, D.; Xing, H. G. Enhancement-Mode Ga_2O_3 Vertical Transistors With Breakdown Voltage >1 kV. *IEEE Electron Device Lett.* **2018**, *39*, 869–872.
(46) Li, W.; Nomoto, K.; Hu, Z.; Jena, D.; Xing, H. G. Field-Plated Ga_2O_3 Trench Schottky Barrier Diodes With a $BV^2/R_{on,sp}$ of up to 0.95 GW/cm^2. *IEEE Electron Device Lett.* **2020**, *41*, 107–110.
(47) Leach, J. H.; Udwary, K.; Rumsey, J.; Dodson, G.; Splawn, H.; Evans, K. R. Halide vapor phase epitaxial growth of β-Ga_2O_3 and α-Ga_2O_3 films. *APL Mater.* **2019**, *7*, 022504.
(48) Vogt, P.; Brandt, O.; Riechert, H.; Lähnemann, J.; Bierwagen, O. Metal-Exchange Catalysis in the Growth of Sesquioxides: Towards Heterostructures of Transparent Oxide Semiconductors. *Phys. Rev. Lett.* **2017**, *119*, 196001.
(49) Vogt, P.; Mauze, A.; Wu, F.; Bonef, B.; Speck, J. S. Metal-oxide catalyzed epitaxy (MOCATAXY): the example of the O plasma-assisted molecular beam epitaxy of β-$(Al_xGa_{1-x})_2O_3$/β-Ga_2O_3 heterostructures. *Appl. Phys. Express* **2018**, *11*, 115503.
(50) Mauze, A.; Zhang, Y.; Itoh, T.; Wu, F.; Speck, J. S. Metal oxide catalyzed epitaxy (MOCATAXY) of β-Ga_2O_3 films in various orientations grown by plasma-assisted molecular beam epitaxy. *APL Mater.* **2020**, *8*, 021104.
(51) Mazzolini, P.; Falkenstein, A.; Wouters, C.; Schewski, R.; Markurt, T.; Galazka, Z.; Martin, M.; Albrecht, M.; Bierwagen, O. Substrate-orientation dependence of β-Ga_2O_3 (100), (010), (001), and $(\bar{2}01)$ homoepitaxy by indium-mediated metal-exchange catalyzed molecular beam epitaxy (MEXCAT-MBE). *APL Mater.* **2020**, *8*, 011107.
(52) Vogt, P.; Hensling, F. V. E.; Azizie, K.; Chang, C. S.; Turner, D.; Park, J.; McCandless, J. P.; Paik, H.; Bocklund, B. J.; Hoffman, G.; Bierwagen, O.; Jena, D.; Xing, H. G.; Mou, S.; Muller, D. A.; Shang, S.-L.; Liu, Z.-K.; Schlom, D. G. Adsorption-controlled growth of Ga_2O_3 by suboxide molecular-beam epitaxy. *APL Mater.* **2021**, *9*, 031101.
(53) Amano, H.; Sawaki, N.; Akasaki, I.; Toyoda, Y. Metalorganic vapor phase epitaxial growth of a high quality GaN film using an AlN buffer layer. *Appl. Phys. Lett.* **1986**, *48*, 353–355.
(54) Hiramatsu, K.; Itoh, S.; Amano, H.; Akasaki, I.; Kuwano, N.; Shiraishi, T.; Oki, K. Growth mechanism of GaN grown on sapphire with A1N buffer layer by MOVPE. *J. Cryst. Growth* **1991**, *115*, 628–633.
(55) Jacko, M. G.; Price, S. J. W. The Pyrolysis of Trimethyl Gallium. *Can. J. Chem.* **1963**, *41*, 1560–1567.

(56) Shenai-Khatkhate, D. V.; Goyette, R. J.; DiCarlo Jr., R. L.; Dripps, G. Environment, health and safety issues for sources used in MOVPE growth of compound semiconductors. *J. Cryst. Growth* **2004**, *272*, 816–821.
(57) Alema, F.; Hertog, B.; Osinsky, A.; Mukhopadhyay, P.; Toporkov, M.; Schoenfeld, W. V. Fast growth rate of epitaxial β–Ga_2O_3 by close coupled showerhead MOCVD. *J. Cryst. Growth* **2017**, *475*, 77–82.
(58) Leedy, K. D.; Chabak, K. D.; Vasilyev, V.; Look, D. C.; Mahalingam, K.; Brown, J. L.; Green, A. J.; Bowers, C. T.; Crespo, A.; Thomson, D. B.; Jessen, G. H. Si content variation and influence of deposition atmosphere in homoepitaxial Si-doped β-Ga_2O_3 films by pulsed laser deposition. *APL Mater.* **2018**, *6*, 101102.
(59) Mauze, A.; Zhang, Y.; Itoh, T.; Ahmadi, E.; Speck, J. S. Sn doping of (010) β-Ga_2O_3 films grown by plasma-assisted molecular beam epitaxy. *Appl. Phys. Lett.* **2020**, *117*, 222102.
(60) Zhang, Y.; Feng, Z.; Karim, M. R.; Zhao, H. High-temperature low-pressure chemical vapor deposition of β-Ga_2O_3. *J. Vac. Sci. Technol. A* **2020**, *38*, 050806.
(61) Bhattacharyya, A.; Ranga, P.; Roy, S.; Ogle, J.; Whittaker-Brooks, L.; Krishnamoorthy, S. Low temperature homoepitaxy of (010) β-Ga_2O_3 by metalorganic vapor phase epitaxy: Expanding the growth window. *Appl. Phys. Lett.* **2020**, *117*, 142102.
(62) Chou, T.-S.; Seyidov, P.; Bin Anooz, S.; Grüneberg, R.; Tran, T. T. V.; Irmscher, K.; Albrecht, M.; Galazka, Z.; Schwarzkopf, J.; Popp, A. Fast homoepitaxial growth of (100) β-Ga_2O_3 thin films via MOVPE. *AIP Adv.* **2021**, *11*, 115323.
(63) Alema, F.; Zhang, Y.; Osinsky, A.; Orishchin, N.; Valente, N.; Mauze, A.; Speck, J. S. Low 10^{14} cm^{-3} free carrier concentration in epitaxial β-Ga_2O_3 grown by MOCVD. *APL Mater.* **2020**, *8*, 021110.
(64) Neal, A. T.; Mou, S.; Rafique, S.; Zhao, H.; Ahmadi, E.; Speck, J. S.; Stevens, K. T.; Blevins, J. D.; Thomson, D. B.; Moser, N.; Chabak, K. D.; Jessen, G. H. Donors and Deep Acceptors in β-Ga_2O_3. *Appl. Phys. Lett.* **2018**, *113*, 062101.
(65) Neal, A. T.; Mou, S.; Lopez, R.; Li, J. V.; Thomson, D. B.; Chabak, K. D.; Jessen, G. H. Incomplete Ionization of a 110 meV Unintentional Donor in β-Ga_2O_3 and its Effect on Power Devices. *Sci. Rep.* **2017**, *7*, 13218.
(66) Mu, S.; Wang, M.; Varley, J. B.; Lyons, J. L.; Wickramaratne, D.; Van de Walle, C. G. Role of carbon and hydrogen in limiting n-type doping of monoclinic $(Al_xGa_{1-x})_2O_3$. *Phys. Rev. B* **2022**, 105, 155201.

Table Caption

Table 1. Summary of MOCVD (010) β-Ga_2O_3 film growth conditions. Listed parameters include growth temperature, chamber pressure, silane, TMGa, and O_2 flow rates, and growth duration. Film thickness, growth rate, carrier concentration and mobility are measured for each sample.

Figure Captions

Figure 1. Surface view FESEM images of β-Ga_2O_3 films grown at different growth temperature: (a) 700 ℃ (Sample #310), (b) 880 ℃ (Sample #307), and (c) 950 ℃ (Sample #309). The TMGa molar flow and O_2 flow rate was set at 58 μmol/min and 800 SCCM, respectively. The chamber pressure was set at 60 Torr. The corresponding surface AFM images with RMS roughness values are shown in (d-f).

Figure 2. Surface view FESEM images of β-Ga_2O_3 films grown at different chamber pressure: (a) 20 torr (Sample #314), (b) 60 torr (Sample #313), and (c) 100 torr (Sample #315). The TMGa molar flow and O_2 flow rate was set at 58 μmol/min and 800 SCCM, respectively. The growth temperature was set at 880 °C. The corresponding surface AFM images with RMS roughness values for samples grown at 60 torr and 100 torr are shown in (d) and (e).

Figure 3. Surface view FESEM images of β-Ga_2O_3 films grown at different TMGa molar flow rate: (a) 48 μmol/min (Sample #320), (b) 58 μmol/min (Sample #316), (c) 87 μmol/min (Sample #322), and (d) 116 μmol/min (Sample #319). The O_2 flow rate was set at 800 SCCM. The growth temperature and chamber pressure was set at 950 ℃ and 60 torr, respectively. The corresponding surface AFM images with RMS roughness values are shown in (e-h).

Figure 4. Surface view FESEM images of β-Ga_2O_3 films grown at different O_2 flow rate: (a) 500 SCCM (Sample #321), (b) 800 SCCM (Sample #322), and (c) 1000 SCCM (Sample #323). The TMGa molar flow rate was set at 87 μmol/min. The growth temperature and

chamber pressure was set at 950 ℃ and 60 torr, respectively. The corresponding surface AFM images with RMS roughness values are shown in (d-f).

Figure 5. Top view FESEM images of MOCVD grown (010) β-Ga_2O_3 thin film with growth rate of 2.95 μm/hr and room temperature mobility of 190 cm^2/vs (Sample #329): (a) large field of view; and (b) high magnification. (c) The corresponding AFM image of the same β-Ga_2O_3 sample.

Figure 6. Mobility data of (010) β-Ga_2O_3 homoepitaxial thin films from this work (TMGa) as compared to previously reported data: room temperature electron mobility vs. electron concentration of β-Ga_2O_3 films grown by different growth techniques. The corresponding growth rates are listed.

Figure 7. (a) Charge carrier density; and (b) measured and fitted temperature-dependent carrier mobility of the MOCVD (010) β-Ga_2O_3 homoepitaxial thin film grown using TMGa as Ga precursor.

Figure 8. Quantitative SIMS impurity depth profiles of the MOCVD (010) β-Ga_2O_3 homoepitaxial thin film grown using TMGa as Ga precursor (Sample #329). SIMS detection limits for each element in this measurement are listed. The asterisks in the legend on H and Cl mean that the extracted average concentration of H and Cl was at the detection limit for H and Cl, respectively.

Table 1

Sample ID	TMGa (μmol/min)	O_2 (SCCM)	Pressure (torr)	Temperature (°C)	Silane (nmol/min)	Duration (min)	Thickness (μm)	Growth Rate (μm/h)	Carrier Concentration (cm^{-3})	Hall Mobility ($cm^2/V{\cdot}s$)
#309	58	800	60	950	0.11	30	1.34	2.68	4.24×10^{16}	163
#307	58	800	60	880	0.11	30	1.42	2.84	-	-
#310	58	800	60	700	0.11	30	1.09	2.18	-	-
#314	58	800	20	950	0.0275	60	3.29	3.29	-	-
#313	58	800	60	950	0.0275	60	2.86	2.86	-	-
#315	58	800	100	950	0.0275	60	1.57	1.57	4.50×10^{16}	134
#311	58	800	60	950	0.0275	60	2.36	2.36	-	-
#316	58	800	60	950	0.11	60	2.59	2.59	-	-
#329	58	800	60	950	0.0496	60	2.95	2.95	1.80×10^{16}	190
#326	58	800	60	950	0.248	60	3.05	3.05	6.01×10^{16}	171
#327	58	800	60	950	1.32	60	2.92	2.92	3.22×10^{17}	142
#335	58	800	60	950	6.614	60	2.68	2.68	1.85×10^{18}	114
#336	58	800	60	950	33.86	60	2.67	2.67	1.06×10^{19}	95
#337	58	800	60	950	166.43	60	3.18	3.18	3.80×10^{19}	93
#330	58	500	60	950	0.0496	60	2.78	2.78	-	-
#320	48	800	60	950	0.089	70	2.75	2.36	-	-
#322	87	800	60	950	0.248	28	2.52	5.4	-	-
#319	116	800	60	950	0.44	16	1.79	6.71	-	-
#321	87	500	60	950	0.248	28	2.91	6.24	-	-
#323	87	1000	60	950	0.248	28	2.22	4.76	-	-
#333	87	800	60	950	0.11	28	2.37	5.08	-	-
#334	87	800	60	950	1.14	28	2.41	5.16	-	-

Figure 1

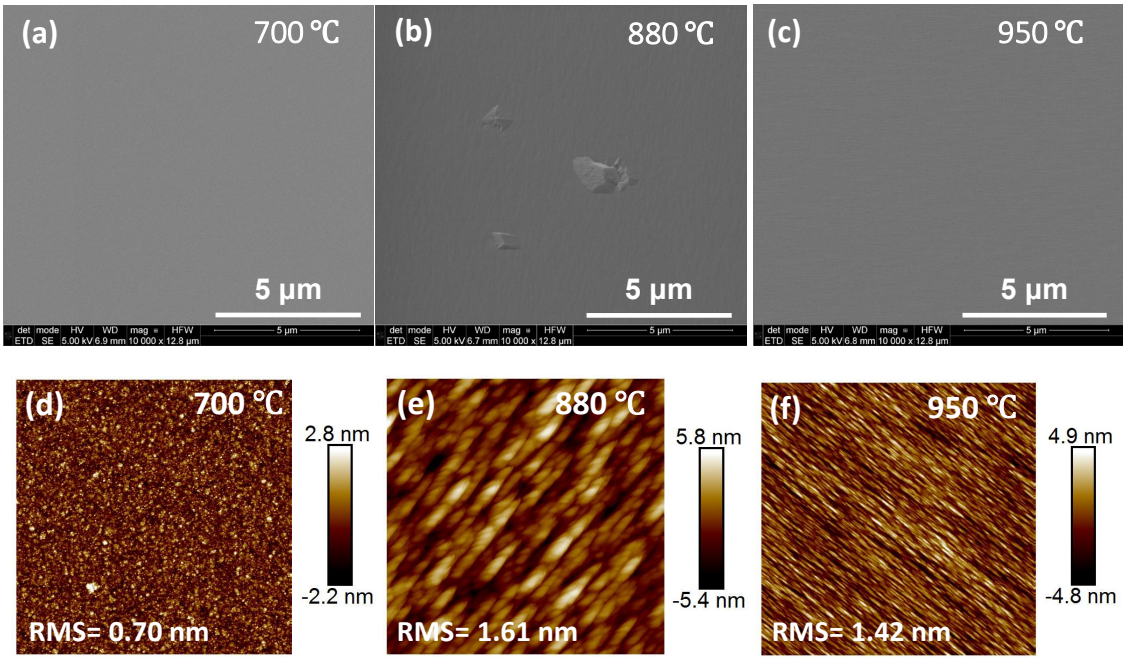
(a)
700 ℃
5 μm
(b)
880 ℃
5 μm
(c)
950 ℃
5 μm
(d)
700 ℃
2.8 nm
-2.2 nm
RMS= 0.70 nm
(e)
880 ℃
5.8 nm
-5.4 nm
RMS= 1.61 nm
(f)
950 ℃
4.9 nm
-4.8 nm
RMS= 1.42 nm

Figure 2

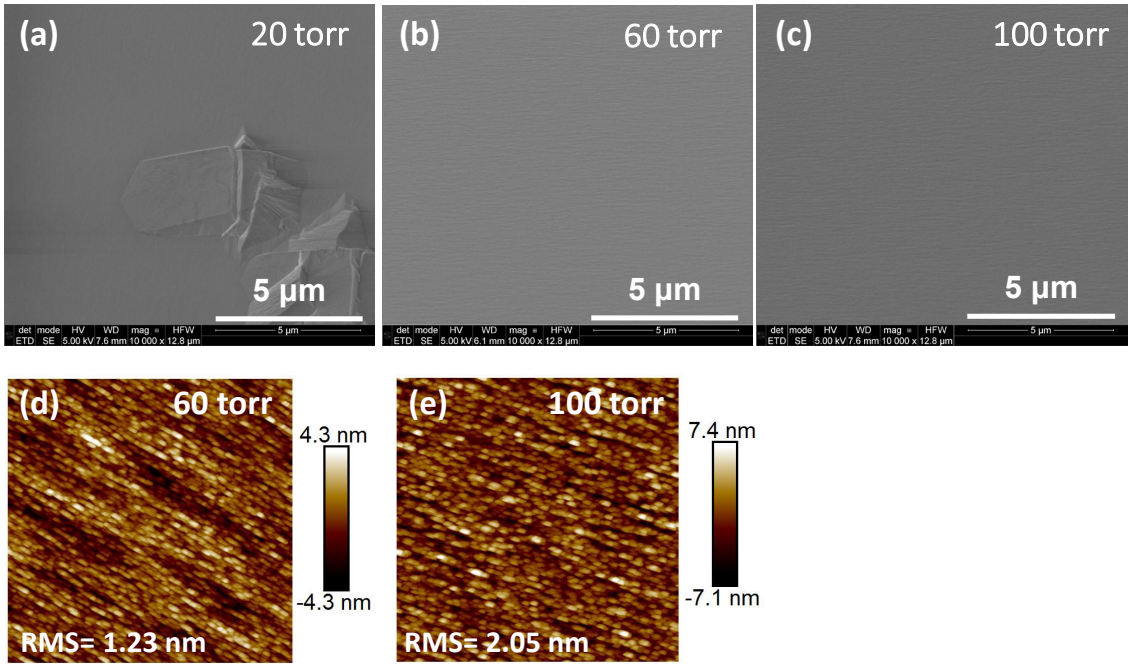
(a)
20 torr
5 μm
(b)
60 torr
5 μm
(c)
100 torr
5 μm
(d)
60 torr
4.3 nm
-4.3 nm
RMS= 1.23 nm
(e)
100 torr
7.4 nm
-7.1 nm
RMS= 2.05 nm

Figure 3

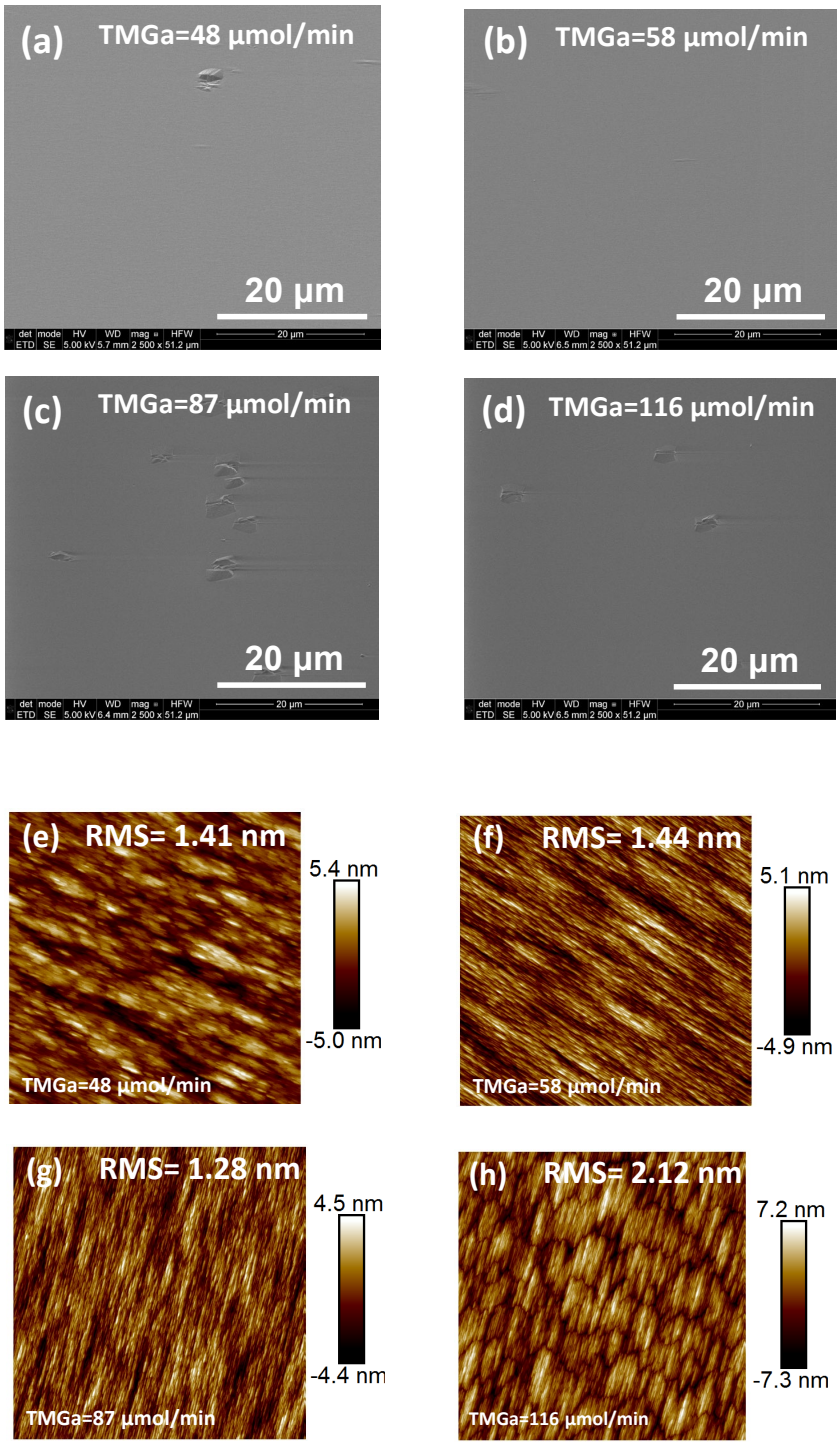
(a) TMGa=48 µmol/min
20 µm
(b) TMGa=58 µmol/min
20 µm
(c) TMGa=87 µmol/min
20 µm
(d) TMGa=116 µmol/min
20 µm
(e) RMS= 1.41 nm
5.4 nm
-5.0 nm
TMGa=48 µmol/min
(f) RMS= 1.44 nm
5.1 nm
-4.9 nm
TMGa=58 µmol/min
(g) RMS= 1.28 nm
4.5 nm
-4.4 nm
TMGa=87 µmol/min
(h) RMS= 2.12 nm
7.2 nm
-7.3 nm
TMGa=116 µmol/min

Figure 4

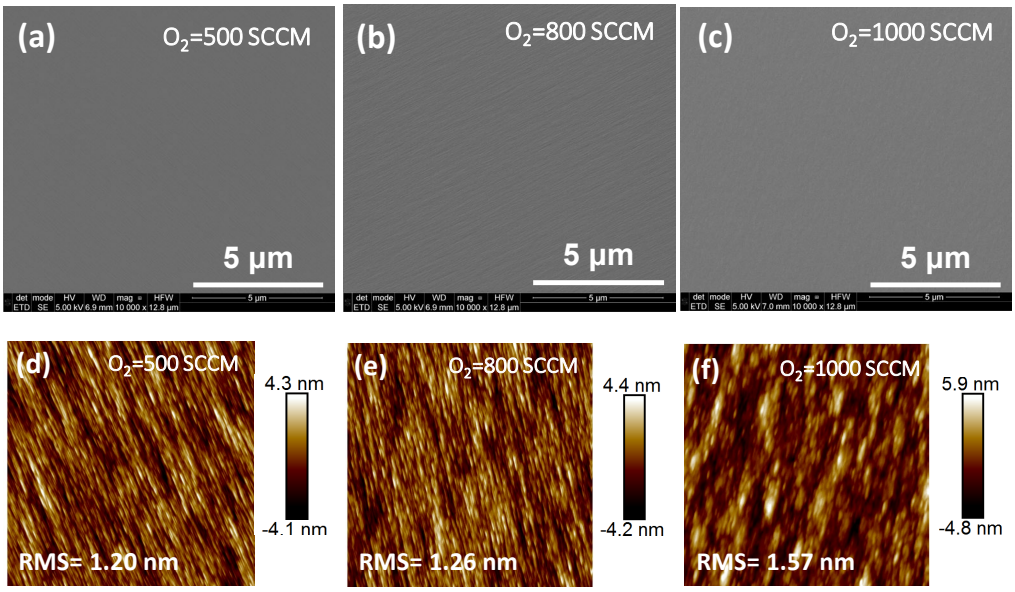
(a)
O_2=500 SCCM
5 µm
(b)
O_2=800 SCCM
5 µm
(c)
O_2=1000 SCCM
5 µm
(d)
O_2=500 SCCM
4.3 nm
-4.1 nm
RMS= 1.20 nm
(e)
O_2=800 SCCM
4.4 nm
-4.2 nm
RMS= 1.26 nm
(f)
O_2=1000 SCCM
5.9 nm
-4.8 nm
RMS= 1.57 nm

Figure 5

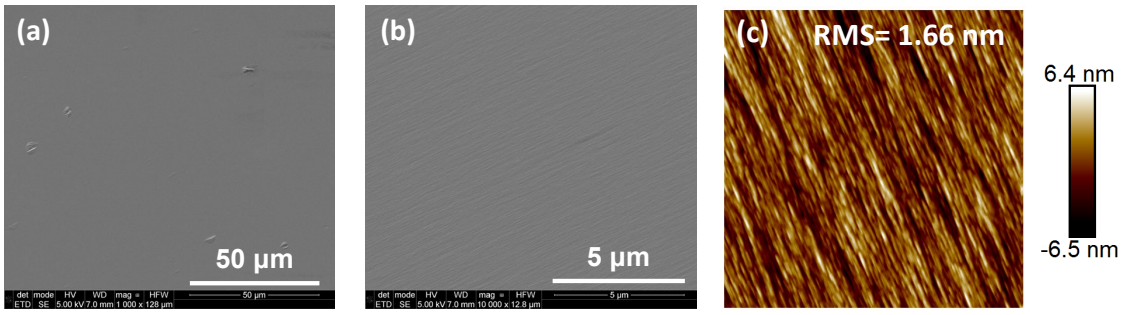

Figure 6

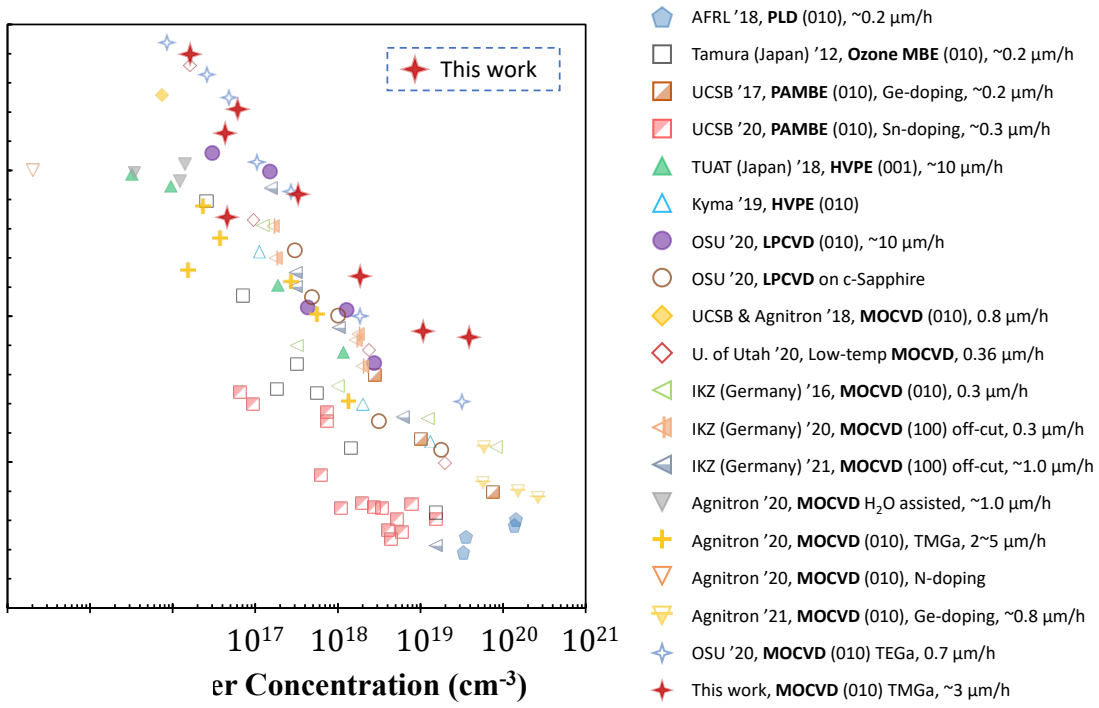
This work
10^{17} 10^{18} 10^{19} 10^{20} 10^{21}
er Concentration (cm^{-3})
AFRL '18, **PLD** (010), ~0.2 µm/h
Tamura (Japan) '12, **Ozone MBE** (010), ~0.2 µm/h
UCSB '17, **PAMBE** (010), Ge-doping, ~0.2 µm/h
UCSB '20, **PAMBE** (010), Sn-doping, ~0.3 µm/h
TUAT (Japan) '18, **HVPE** (001), ~10 µm/h
Kyma '19, **HVPE** (010)
OSU '20, **LPCVD** (010), ~10 µm/h
OSU '20, **LPCVD** on c-Sapphire
UCSB & Agnitron '18, **MOCVD** (010), 0.8 µm/h
U. of Utah '20, Low-temp **MOCVD**, 0.36 µm/h
IKZ (Germany) '16, **MOCVD** (010), 0.3 µm/h
IKZ (Germany) '20, **MOCVD** (100) off-cut, 0.3 µm/h
IKZ (Germany) '21, **MOCVD** (100) off-cut, ~1.0 µm/h
Agnitron '20, **MOCVD** H_2O assisted, ~1.0 µm/h
Agnitron '20, **MOCVD** (010), TMGa, 2~5 µm/h
Agnitron '20, **MOCVD** (010), N-doping
Agnitron '21, **MOCVD** (010), Ge-doping, ~0.8 µm/h
OSU '20, **MOCVD** (010) TEGa, 0.7 µm/h
This work, **MOCVD** (010) TMGa, ~3 µm/h

Figure 7

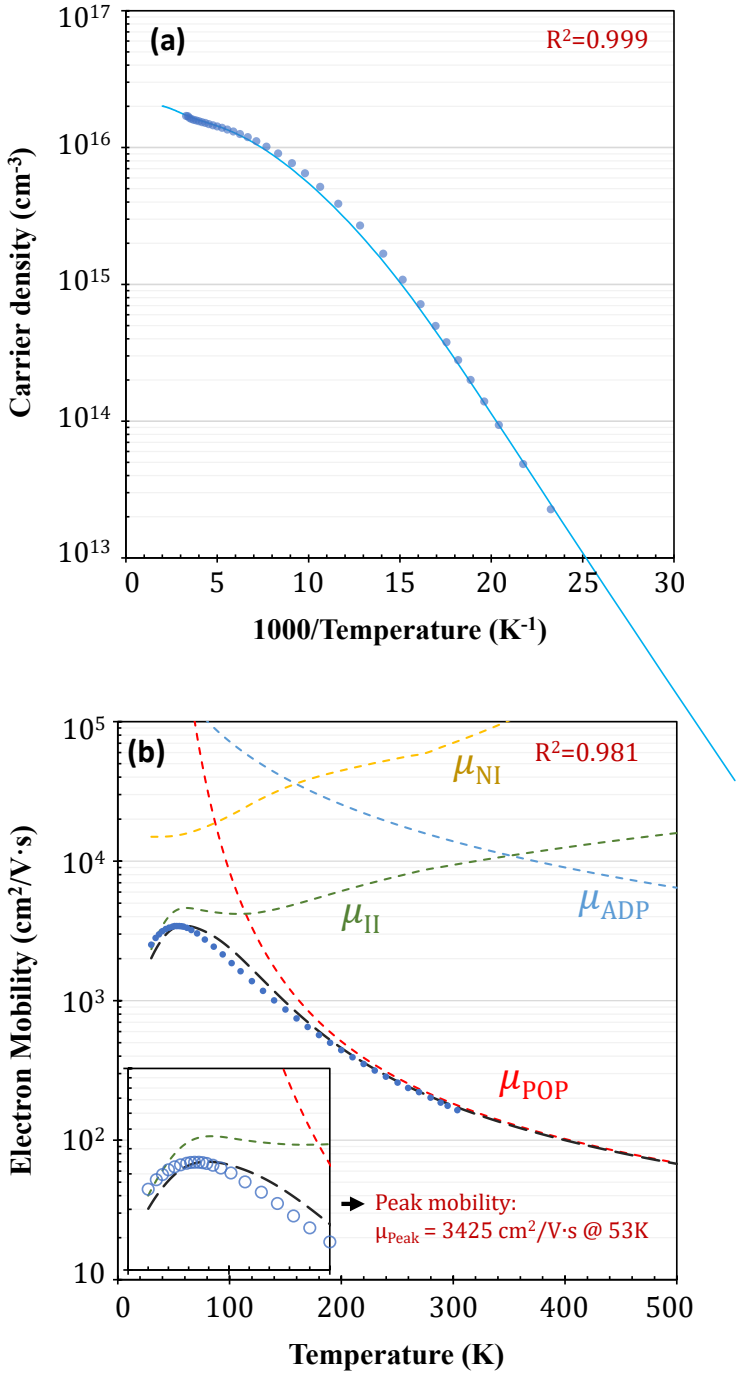
(a)
R²=0.999
Carrier density (cm⁻³)
1000/Temperature (K⁻¹)
(b)
R²=0.981
μNI
μII
μADP
μPOP
Peak mobility:
μPeak = 3425 cm²/V·s @ 53K
Electron Mobility (cm²/V·s)
Temperature (K)

Figure 8

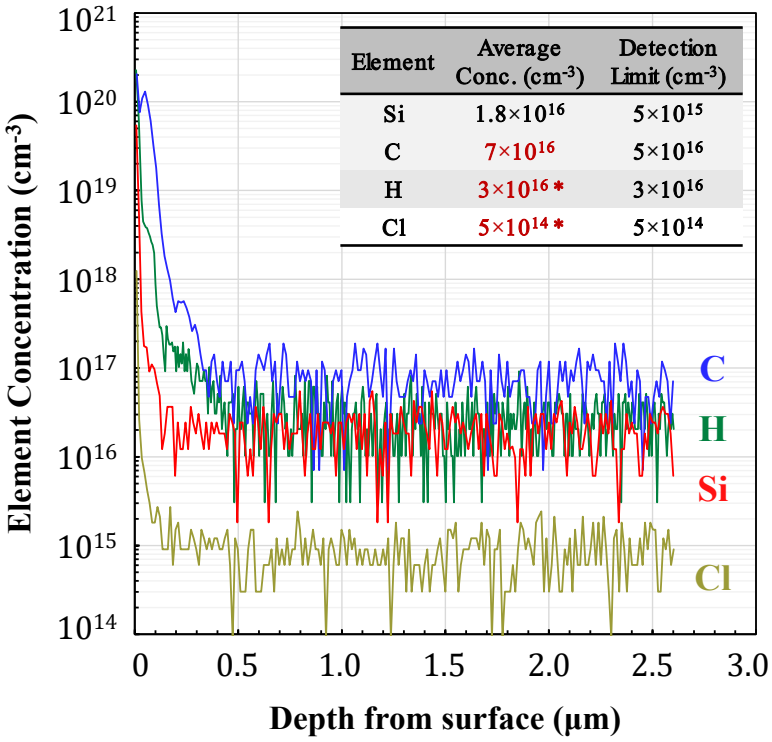
Element
Average Conc. (cm-3)
Detection Limit (cm-3)
Si
1.8×10^16
5×10^15
C
7×10^16
5×10^16
H
3×10^16 *
3×10^16
Cl
5×10^14 *
5×10^14
Element Concentration (cm-3)
10^21
10^20
10^19
10^18
10^17
10^16
10^15
10^14
0
0.5
1.0
1.5
2.0
2.5
3.0
Depth from surface (µm)
C
H
Si
Cl